vulcanhammer.info
February 2023

DOI: 10.13140/RG.2.2.22395.18727

Development of a Parametric Model for the Simulation of Impact-Vibration Pile Driving Equipment

Don C. Warrington, PhD., P.E.
University of Tennessee at Chattanooga
Department of Mechanical Engineering

Impact-vibration pile driving equipment has been an important part of vibratory pile driving equipment since the early years of development. In the 1960's the VNIIstroidormash institute in Moscow developed a series of impact-vibration hammers; however, the development of these hammers was stopped in favour of the diesel hammers. The emergence of the need to convert construction equipment to electric power due to environmental considerations reopens the possibility that these hammers may once again need to be considered to drive piles, as the original impact-vibration hammers (in common with their early vibratory counterparts) were powered using specialised electric motors. A model is first developed to simulate the mechanical working of these hammers, followed by comparison to actual designs. The results are generally in line with the original tests (to the extent the results are known) but variances are noted and discussed. Some suggestions for forward movement on the design of this equipment are set forth.

Keywords: impact-vibration, vibratory, pile driving, VNIIstroidormash, differential equations, Runge-Kutta

Background

General History of Impact-Vibration Hammers in the Soviet Union

The effort to develop vibratory pile driving equipment–along with other types of vibrating equipment–was a major effort in the Soviet Union during and in the years following the "Great Patriotic War" (World War II.) For most outside of the country the realisation that the Soviets had developed vibratory pile drivers came with the presentation of Barkan (1957). The development of these machines–along with the impact-vibration ones–is more thoroughly discussed in Erofeev, Smorodinov, Fedorov, Vyazovkii, and Villumsen (1985); Rebrik (1966); Savinov and Luskin (1960); Tseitlin, Verstov, and Azbel (1987).

The development of impact-vibration equipment began with a rather commonplace realisation: if you didn't clamp the vibrator to the load and didn't have a suspension to apply downward force, it would jump up and down, impacting the same. The earliest impact-vibration hammer was developed by S.A. Tsaplin and is described in brief in Warrington and Erofeev (1995). He began his research in 1949 and first published his results in 1953. A machine associated with Tsaplin was the VMTs-3 impact vibration hammer, shown in Figure 1.

All of the basic elements of subsequent impact-vibration hammers can be seen in this machine. The two cylinders at the top house the motor-eccentric ram assembly. Although the suspension springs connect a static weight to a vibrating one, the purpose of both is entirely different. The vibrating weight, instead of transmitting the vibrations directly to the pile, impacts the pile head (generally via an anvil/cushion arrangement) while the static weight rests on the pile, adapts the machine to the pile and prevents excessive upward motion in the vibrating part.

Warrington and Erofeev (1995) discuss much of the subsequent development of impact-vibration hammers at VNIIstroidormash, the All-Union Scientific Research Institute of Construction and Road-Building Machinery, based in Moscow. One machine not mentioned in this paper was the S-402, which was a small prototype machine shown in Figure 2. A successor machine to this will be analysed in detail in this paper. As was the case with the VMTs-3, all of the basic elements of impact-vibration hammers are present here.

The machines in Figures 1 and 2 have the same basic construction. The ram is not simply a weight moved by external forces (usually fluid pressure) but has an internal electric mo-

I must once again acknowledge my debt to my friend and VNIIstroidormash's senior pile driving equipment designer, Lev Viktorovich Erofeev, for furnishing me with the drawings and specifications for the hammers reviewed in this article. It was his desire for this effort not to be forgotten and it is my desire for that to be fulfilled, now that the time for this design may be more favourable than it was in his day and for most of my career.

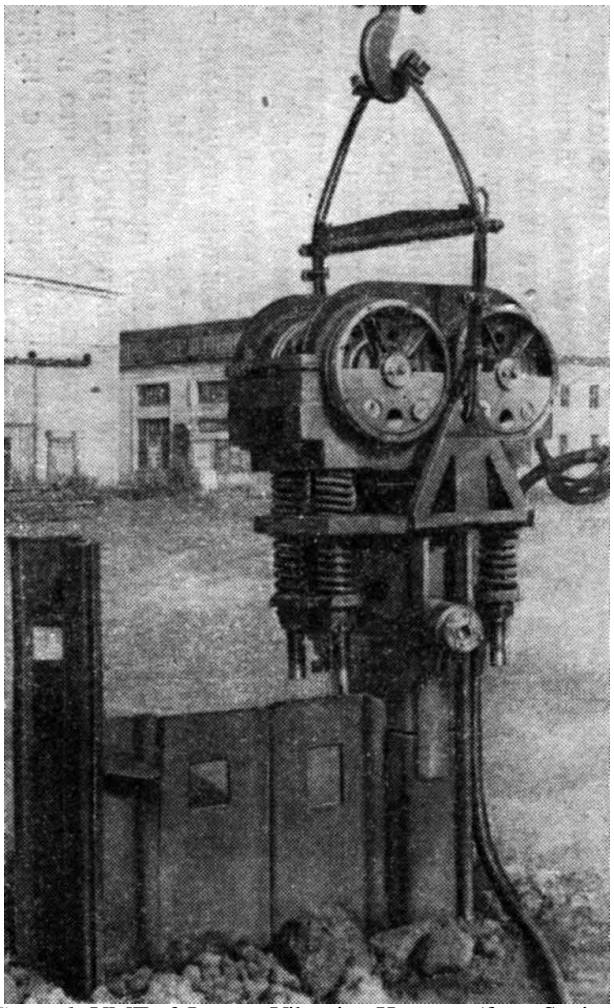

Figure 1. VMTs-3 Impact-Vibration Hammer (from Savinov and Luskin (1960))

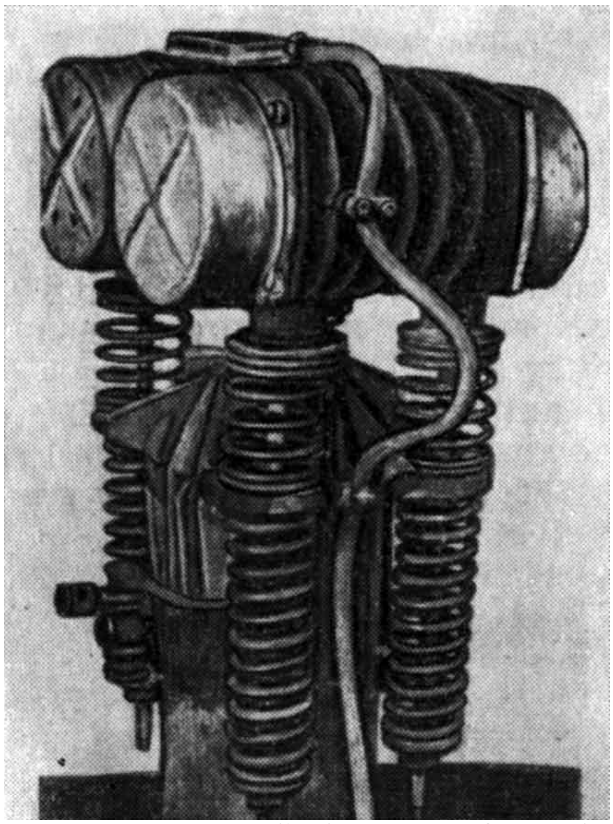

Figure 2. S-402 Impact-Vibration Hammer (from Savinov and Luskin (1960))

tor which turns the shaft and the two eccentrics which are mounted at each end of the shaft. The internal construction of this is shown in Figure 3.

In this construction, the eccentrics are directly driven by the motor. Most of these machines had the eccentrics to "self-synchronise" through the amplitude of the ram, rather than to have a gear driven system such as is the case with most vibratory drivers. A similar concept was used with the Tünkers vibratory drivers. The electric motors were a special "APOVV" type, which went through further refinement in order to prevent the disintegration and shorting of the wiring (Warrington and Erofeev (1995).)

There were several variations on the internal construction of the machines, and especially that of the frame; one example is the S-834. A cutaway view of the lower frame is shown in Figure 4. How this interfaced with the pile is shown in Figure 5. It is evident from these figures and Figure 8 that an important objective of these hammers was to drive

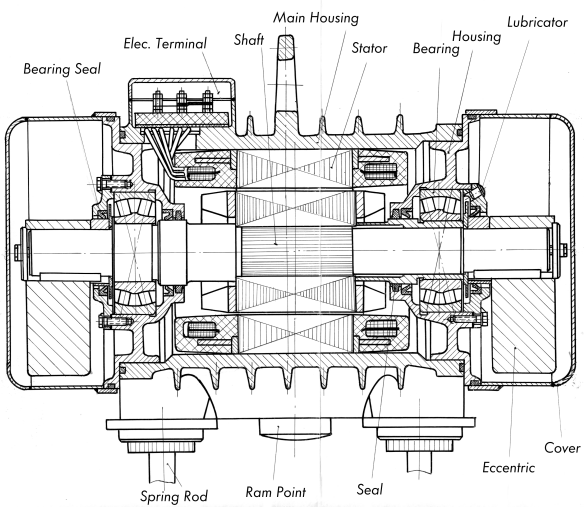

Figure 3. Internal Construction of Impact-Vibration Ram, S-834 (from Petrushkin, Friedman, and Morgailo (1964))

concrete piles. The adjustable opening shown in Figure 4 is an interesting concept, as anyone who has dealt with driving accessories will attest. How well it worked in practice is not clear. Also, raising the pile using the hammer frame, as shown in Figure 5, is not an uncommon practice in impact pile driving, although the schematic rig shown in Figure 20 (and the excavator mast setup in Figure 21) show a sheave setup for a pile line.

A parallel effort also took place in Leningrad (St. Petersburg) and this is described by Tseitlin et al. (1987). Although the theoretical/numerical modelling techniques developed here will be featured in this study, these designs will not be discussed further.

Need for Impact-Vibration Hammers

As described by Warrington (1992), vibratory hammers operate under the principle of reducing the resistance of the soil, which allows the vibrator and pile to move downward in the soil by the weight of the system. A good deal of this loosening is due to inducing horizontal stresses in soils (Massarsch (2023).) Same stresses tend to be long-lasting, which has complicated the axial capacity estimation of vibrated piles for a long time (Massarsch and Fellenius (2020).) Soils and piles exist that do not respond to purely vibratory action; thus, it is necessary to generate higher forces to move the pile using impacts. This has led to the common practice of using both types of pile driving equipment for the same pile, in addition to the issue of the static axial capacity of impact vs. vibratory driven piles. One purpose of the impact-vibration hammer was to obviate the need for vibratory hammers in some circumstances or even have a driver capable of both modes of operation (see below.) However, around 1970 the Soviet effort was stopped because it was felt that the diesel hammer, which is common for impact pile driving in all parts of the world, would be sufficient to meet the requirement for impact forces.

Impact-vibration hammers have four important advantages which have the potential to bring them back into production and use.

The first is the high blow rate of the hammer. Most of the hammers studied in this paper have an impact frequency of around 480 impacts/minute. It has been noted (although formal studies are sadly lacking) that high blow rate hammers, such as the Super-Vulcan and MKT "B" series hammers, are able to induce continuous movement in the soil–and the soil relaxation that goes with it–by forcing the system to move in a more continuous manner, thus improving soil relaxation and making driving easier. Most diesel hammers, on the other hand, operate around 35-60 impacts/minute, and the soil has more time to set up between blows and make driving more difficult. This phenomenon can also be seen in external combustion hammers.

The second is that they were electrically driven. Until the late 1960's virtually all vibratory hammers had electric motors to turn the eccentrics. Most impact-vibration hammers actually provided direct drive for the eccentrics from the motor, as the Uraga vibratory driver did. Today most vibratory drivers are hydraulically driven. While this has resulted in reliable machines, the growing interest in potentially carbon-free energy for construction equipment has revived interest in electrically driven construction equipment. While it is certainly possible to use "electric over hydraulic" systems, this involves another energy conversion which reduces the energy efficiency of the equipment.

The third is that impact-vibration hammers function by converting rotary energy from the eccentrics into translational impacts on the pile. While the use of mechanical pistons and cylinders is accepted and sound practice for all impact hammers, to do this using translational electric solenoids and other components is not an efficient option. So the possibility of using rotary equipment to produce translational ram motion and impact is an inviting one.

The fourth is that impact-vibration hammers can be made shorter than their purely reciprocating impact counterparts. This will be discussed later in the paper.

Table 1
Impact-Vibration Hammers in this Study

Model	Year	K, kg-m	M, kg	RPM_3	RPM_4	N_{rat}, kW
S-834	1963	5.5	650	950	475	11
S-467M	1965	22.5	1900	980	480	44
S-402A	1966	2.2	284	960	480	2.2
SP-53	1967	221	8000	400	200	50
S-836	1969	14	1400	970	485	26

Information Source for Impact-Vibration Hammers

In the late 1980's and early 1990's Vulcan Iron Works established relationships with institutes and factories in what started out as the Soviet Union and ended up as the Russian Federation. During this time there were several cooperative efforts, such as commissioning the design of fabricated tubular diesel hammers and the sea water pile hammer (Warrington, Nifontov, Erofeev, and Trifonov-Yakovlev (1997).)

Vulcan's interest in Soviet/Russian vibratory technology was limited because of its electric drive and other aspects of its construction. The impact-vibration hammer was intriguing, if not very useful at the time, because of both the electric drive and other aspects of the design of these hammers. Vulcan personnel were able to obtain drawing sets (in varying states of completeness) for five models, which are listed (along with basic specifications) in Table 1. Most of these specifications are drawn from the drawings or accompanying documentation; some of this documentation is directly referenced in the report.

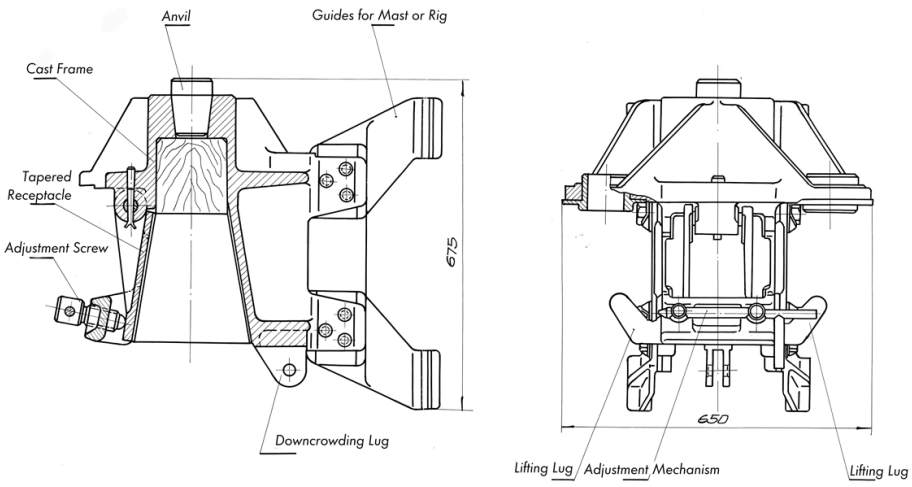

Figure 4. Lower Frame, S-834 (from Petrushkin et al. (1964))

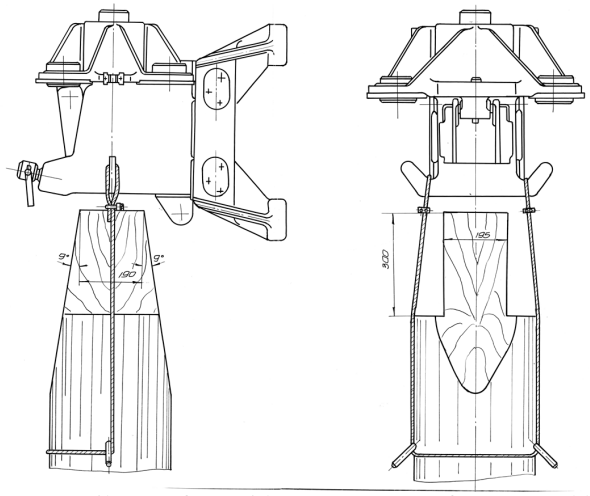

Figure 5. Pile Interface with Frame, S-834 (from Petrushkin et al. (1964))

The S-402A is similar in size to the S-402 shown in Figure 2, but RPM_3 was reduced from 1440 RPM and the eccentric moment was doubled. The models S-834, SP-53 and S-836 are shown in Figures 6, 7 and 8 respectively.

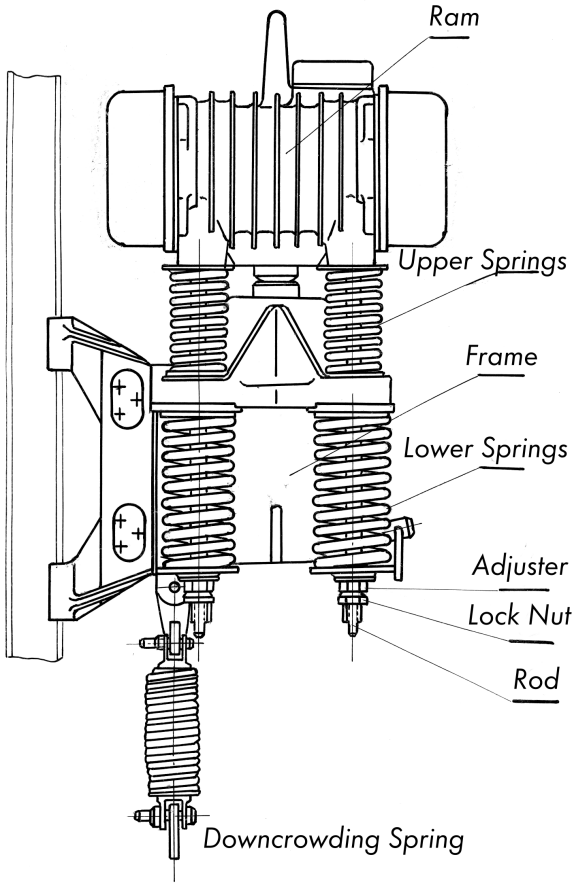

Figure 6. S-834 Impact-Vibration Hammer (from Petrushkin et al. (1964))

Development of the Model and Definition of the Operating Parameters

As the object of this study is to develop and use a mathematical model to simulate the action of impact-vibration hammers, it makes sense to also use this model to discuss the important operating parameters of the machine.

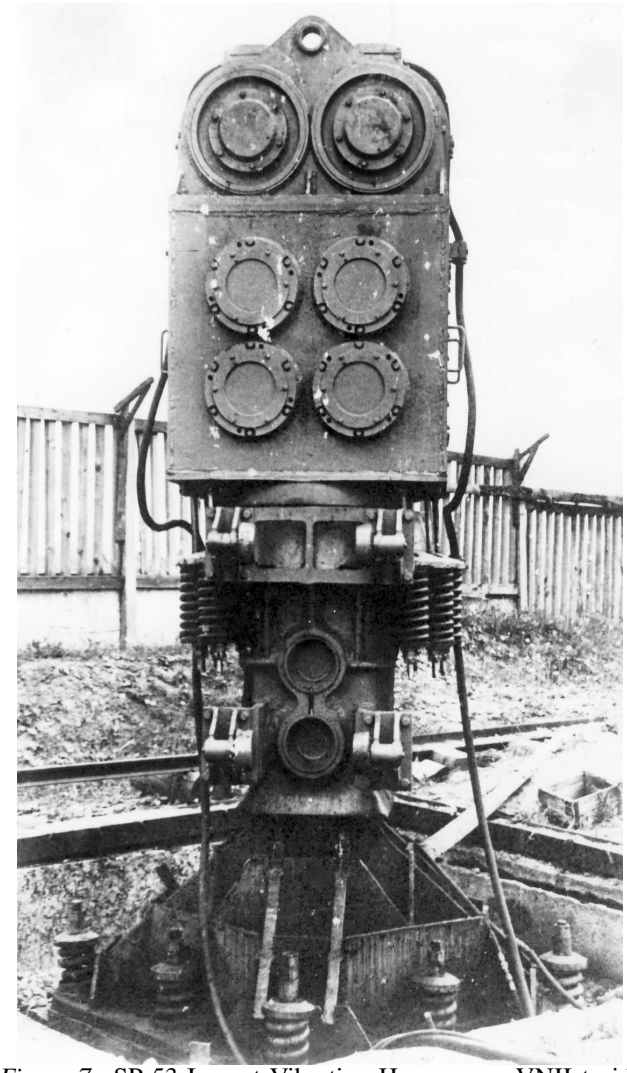

Figure 7. SP-53 Impact-Vibration Hammer on VNIIstroidormash Test Stand (from Warrington and Erofeev (1995))

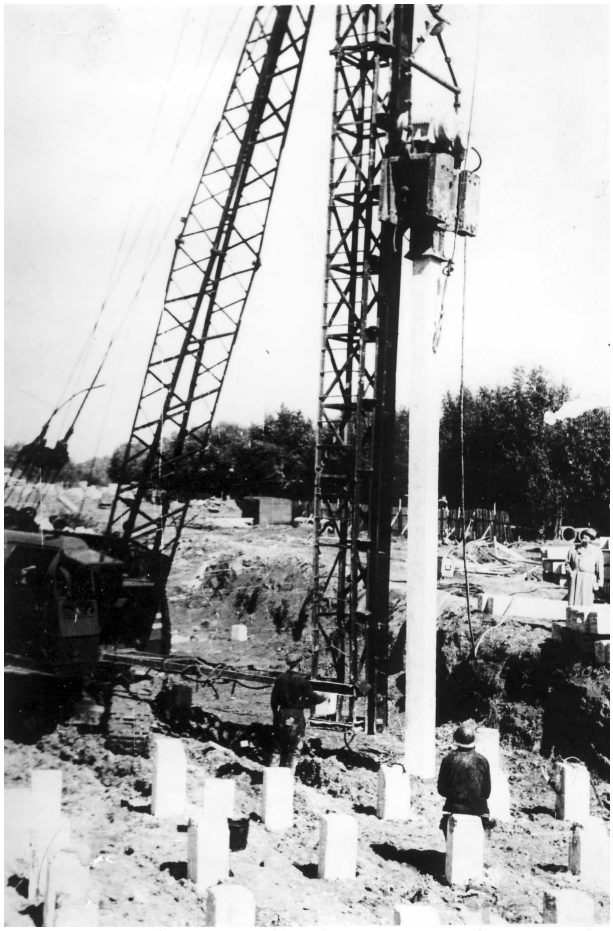

Figure 8. S-836 Impact-Vibration Hammer (from Warrington and Erofeev (1995))

Governing Equations

The governing equations for impact vibration hammers such as are discussed in this paper are given as follows:

$$\frac{d^2}{dt^2}\alpha(t) - \frac{K\cos(\alpha(t))\frac{d^2}{dt^2}x(t)}{I_o} = \frac{T}{I_o} - \frac{K\cos(\alpha(t))g_c}{I_o} \quad (1)$$

and

$$-K\left(\frac{d^2}{dt^2}\alpha(t)\right)\cos(\alpha(t)) + M\frac{d^2}{dt^2}x(t) = Mg_c + Q_{vp} - Z\frac{d}{dt}x(t) - kx(t) - K\left(\frac{d}{dt}\alpha(t)\right)^2\sin(\alpha(t)) \quad (2)$$

A free-body schematic is shown in Figure 9.

The model is based on Tseitlin et al. (1987) and Warrington (2022), and the way the model was rendered parametric–and solved–is very similar to the latter. However, there

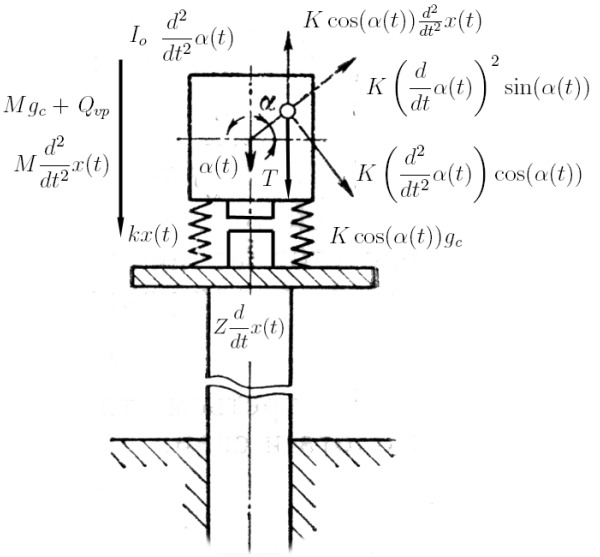

Figure 9. Schematic for Parametric Model for Impact Vibration Hammer (based on Tseitlin et al. (1987); Warrington (2022))

are several important changes from that effort, which are as follows:

1. The effect of gravity, which Warrington (2022) dropped, was returned to the model. Because the machine's impacting part is in flight most of the time, the effect of gravity is more pronounced than it is with the power calculations for vibratory machines. Also, the model of Warrington (2022) was intended to be consistent with earlier models such as Warrington (1994, 2006);

2. The suspension springs were added; and,

3. The viscous damping of the soil was replaced by the impedance of the pile (or more accurately the pile head system.)

These and other aspects of the design/model will be discussed.

Frequencies Affecting Operation

As is the case with virtually any piece of pile driving equipment, impact-vibration hammers are periodic in their operation. With vibratory drivers, the constantly varying torque (Warrington (1994, 2006)) suggested that the rotational speed might likewise vary, and that this variation be significant. Warrington (2022) demonstrated that, if the soil is assumed to act as a viscous damper, this variation is not significant for vibratory hammers with conventional construction of eccentrics, although in the case of difficult soils and rocks this may not be the case.

With impact-vibration hammers variations from purely sinusoidal rotation caused in part by the impact of the vibrating mass have been recognised to be potentially significant in the operation of the equipment. In the early years, with the lack of computational power available to the researchers, an assumption was made that $\frac{d^2}{dt^2}\alpha(t) = 0$. The fact that the machines worked as well as they did was a testament to the basic reasonableness of that assumption, the competence of the researchers and the fact that they were able to build actual working models to verify their results.

The fact remains, however, that for completeness it is necessary to find basic periodic relationships in a system where the angular velocity of the eccentrics is not constant. This was the greatest challenge in the development of this model, and forced the numerical solution of Equations 1 and 2. In any case it is first necessary to define four frequencies that affect the operation of the machine as follows:

• Pendulum frequency of the eccentrics ω_1. This is a function of I_o and K and is given by the equation (Warrington (2022))

$$\omega_1 = \sqrt{\frac{Kg_c}{I_o}} \tag{3}$$

• Natural frequency of the spring-mass system ω_2, given by the equation

$$\omega_2 = \sqrt{\frac{k}{M}} \tag{4}$$

The ratio between the first two frequencies is designated as

$$\eta_4 = \frac{\omega_2}{\omega_1} \tag{5}$$

• Rotational frequency of the eccentrics ω_3. This was to some extent constrained by the frequencies available on synchronous motors (Ivanov-Smoleksky (1982)) and for most of the machines studied varied between 950 and 980 RPM.

• Frequency of the impacts ω_4. One of the important outcomes of impact-vibration design is that ω_4 does not have to equal ω_3. However, for stable, synchronous rotation of the eccentrics, in the absence of a speed reduction system such as was used in the SP-53, it is necessary that ω_4 and ω_3 be integer multiples of each other, thus

$$i = \frac{\omega_3}{\omega_4} \tag{6}$$

Research early in the development of these machines, based on the work of I.G. Rusakov and A.A. Kharkevitch, showed that the relationship between the frequency of impacts and the rotational frequency could be regulated through proper selection of the natural frequency. From this, the following relationship was established:

$$i = \frac{\sqrt{\beta}\omega_3}{2\omega_2} = \frac{\sqrt{\beta}}{2\xi} \tag{7}$$

where

$$\xi = \frac{\omega_2}{\omega_3} \tag{8}$$

One of the main tasks of the model is to verify this relationship for the machines in Table 1. Generally speaking, except for the SP-53, VNIIstroidormash designers designed their machines for $i = 2$. The advantage of enabling the impact mass to "skip" eccentric rotations is that it allows a higher frequency (lower torque) motor relative to a desired frequency of impacts, thus using the suspension as a *de facto* speed reducer. With the SP-53 an actual gear system is used which adds to the expense of the machine and decreases its mechanical efficiency. It should be evident that, given i, β and ω_3 the spring constant k can be computed.

As was the case with Warrington (2022), it was necessary to choose a "fundamental" frequency in order to nondimensionalise the time. The frequency ω_1 was chosen, which leads to the first variable change for Equations 1 and 2, namely

$$\tau = \omega_1 t \tag{9}$$

All frequencies shown here can be expressed either in radians/second (ω) or revolutions/minute (RPM,) which are related as follows:

$$RPM_n = \frac{30\omega_n}{\pi} \tag{10}$$

It is generally more convenient to express these quantities in RPM.

The Torque Ratio and the Effect of Gravity

As was noted earlier, in Warrington (2022) the effect of gravity was ignored. In this system it was considered. One important result of that addition concerned the torque ratio

$$\eta_1 = \frac{T}{Kg_c} \tag{11}$$

At the start of operations, in order to get the eccentrics "over centre" (i.e., past $\alpha = 0$,) it is necessary for the torque to exceed the eccentric moment, or $T > Kg_c$. For purposes of our calculations the torque ratio was set at a minimum of $\eta_1 \geq 1.1$. Implicit in this formulation is that the starting torque at $RPM_3 = 0$ is the same as the steady-state torque at the final value of RPM_3. Most motors of the type used in these machines have a higher starting torque, but for conservatism this was neglected. One of the main differences in this model and that of Tseitlin et al. (1987) or even Warrington (2021) is that, instead of modelling one cycle from computed initial conditions, the machine was started from rest and, assuming a constant torque, the machine assumed the rotational speed the torque could achieve with the load.

The Resistive Impedance of the Pile-Hammer System

The way in which the pile cushion-pile system was modelled in Tseitlin et al. (1987) reflected typical Soviet practice of assuming the pile was a rigid mass, in much the same way as is done with the dynamic formulae. This was a signal weakness in the whole Soviet approach to impact pile driving, especially considering that since Isaacs (1931) wave propagation in piles had been recognised and since Smith (1960) viable numerical methods had been employed to simulate these kinds of effects.

Unfortunately, for a simple parametric model such as is proposed here, coming up with a reasonable model that simulates at least some of these kinds of effects without having to model the entire pile–and propose a soil profile to go with it–has its own problems. The need for a pile hammer to effectively interact with a wide variety of pile-soil systems is one of the great challenges in the design of impact pile hammers, especially with impact-vibration hammers whose performance is dependent upon the interaction of the hammer with what it is striking. (Diesel hammers also have this problem; it was the reason why the WEAP program (Goble and Rausche (1976)) was such an advance in the development of the wave equation.) In the end, after some experimentation, an impedance type of model was adopted. The response of the pile head to impact was simplified to a velocity dependent force based on an effective pile head impedance Z. This is stated non-dimensionally with the constant

$$\zeta = \frac{Z}{M\omega_3} \tag{12}$$

and so

$$Z = \zeta M\omega_3 \tag{13}$$

Because the "baseline" frequency is the pendulum frequency, for use with the governing equations the constant was stated as follows:

$$\eta_2 = \frac{Z}{M\omega_1},\ x(\tau) > 0 \wedge \frac{d}{dt}x(\tau) > 0 \tag{14}$$
$$\eta_2 = 0,\ x(\tau) \leq 0 \vee \frac{d}{dt}x(\tau) < 0$$

and the two can be related as follows:

$$\eta_2 = \zeta\frac{\omega_1}{\omega_3} = \frac{\zeta\xi}{\eta_4} \tag{15}$$

The conditions are included in Equation 14 because the impact takes place at an inextensible interface. One result of a purely impedance based model is the lack of rebound from the pile, which eliminates the stroke speed restoration coefficient R from consideration.

It is worth noting at this point that VNIIstroidormash designers had two limitations in the design of the impacting mass, which included the electric motors:

1. The peak deceleration of the impacting mass n_{impact} was 150 g's. This was based on experiment and is not unreasonable for impact pile driving equipment.

2. The peak impact velocity $V_{1_{max}}$ was to be 2 m/sec.

If we assume that the peak impact force is both a) the product of the impedance of the pile head and the impact velocity and b) the peak deceleration of the ram, we can equate the two as follows

$$ZV_1 = Mn_{impact} \tag{16}$$

and thus

$$n_{impact} = \frac{ZV_1}{M} \tag{17}$$

Combining Equations 12 and 16 yields

$$\zeta = \frac{n_{impact}}{V_1\omega_3} \tag{18}$$

For the range of all of the machines studied except for the S-53, $7 < \zeta < 7.5$, the SP-53 was around 17.5. This determination was useful in setting the trial values of ζ for the studies.

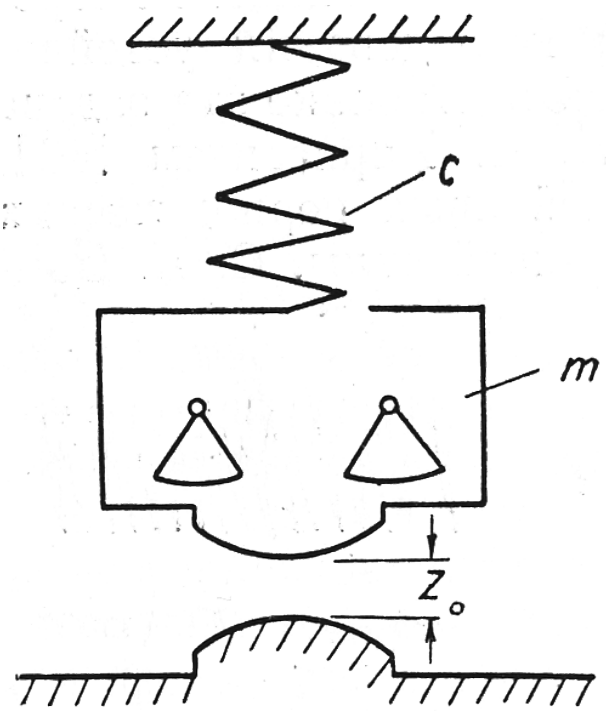

Figure 10. Illustration of Impact Clearance (from Savinov and Luskin (1960))

Clearance and Bias Issues

All impact hammers have a "standard impact point," i.e., a place in the geometry of the machine where the ram, under normal conditions, strikes the top plate, anvil or cushion material and begins imparting impact force to the pile-soil system. This point is necessary to establish what constitutes things such as a full stroke, proper packing of the cushion material, proper timing for either advance upstroke admission or fuel injection/compression/combustion, etc.. Impact-vibration hammers are no exception to this; additionally, the spring suspension makes it possible for the ram, at its own rest position, to be is various positions relative to the rest position of the anvil. From this, it is possible for the rest position of the ram to be somewhere else than the standard impact point dictated by the anvil. This is illustrated in Figure 10; the figure shows that the clearance Z_o is in this case positive and that, at the start of the machine's operation, the ram is floating above the anvil. It is possible for the clearance to be positive, negative or zero, and this is discussed in Warrington and Erofeev (1995).

In order to produce a given clearance, it is necessary to adjust the springs to induce a certain position. This force will be referred to as the bias force of the springs, designated as Q_{vp}; inspection of Figure 6 will show that this bias force is adjustable, as it is in all of the machines under consideration. We can define the ratio between the bias force and the weight of the ram as follows:

$$\eta_5 = \frac{Q_{vp}}{Mg_c} \tag{19}$$

The problem is that, for values of $Z_o \leq 0$, there is not a one-to-one correspondence between Q_{vp} and Z_o. In fact, for any value of $-1 \leq \eta_5 \leq 0$, $Z_o = 0$ by static equilibrium. (This statement assumes that negative clearance is induced by a positive downward force of the springs and not simply the gravitational effect on the ram.)

VNIIstroidormash designers settled on zero clearance; however, this leaves us with the question of the bias force. Runs of the model showed that the model ran most closely to the original specifications when $\eta_5 = -1$, and this was used for most of the model runs.

Dynamic Force of Eccentrics

As is the case with vibratory drivers, the rotating eccentrics exert a sinusoidal dynamic force on the ram. If the ram is considered without the effect of the suspension springs or impact, the peak acceleration is given as

$$n = \frac{F_{dyn}}{Mg_c} \tag{20}$$

where

$$F_{dyn} = K\omega_3^2 \tag{21}$$

As is the case with the impedance, this dimensionless variable can be expressed in terms of the pendulum frequency,

$$\eta_3 = \frac{K\omega_1^2}{Mg_c} \tag{22}$$

and the two can be related as follows:

$$\eta_3 = n\left(\frac{\omega_1}{\omega_3}\right)^2 \tag{23}$$

Making the Governing Equations Parametric, and Their Solution

Rewriting the Governing Equations

Now that we have defined important dimensionless parameters, we can proceed with applying these to Equations 1 and 2 and applying a solution method. Equation 9 made the time dimensionless, and it is necessary to do the same with the displacement. This is done as follows:

$$X(\tau) = \frac{x(\tau){\omega_1}^2}{g_c} \tag{24}$$

This done, and applying all other dimensionless coefficients, we can restate Equations 1 and 2 as follows:

$$\frac{d^2}{d\tau^2}\alpha(\tau) - \cos(\alpha(\tau))\frac{d^2}{d\tau^2}X(\tau) = \eta_1 - \cos(\alpha(\tau)) \tag{25}$$

$$-\left(\frac{d^2}{d\tau^2}\alpha(\tau)\right)\cos(\alpha(\tau))\eta_3 + \frac{d^2}{d\tau^2}X(\tau) = 1 + \eta_5 - \eta_2\frac{d}{d\tau}X(\tau) - {\eta_4}^2 X(\tau) - \left(\frac{d}{d\tau}\alpha(\tau)\right)^2 \sin(\alpha(\tau))\eta_3 \tag{26}$$

As was the case with Warrington (2022), we will use a fourth-order Runge-Kutta solution. Since it is necessary to define these equations as a series of first-order derivatives we will, as in that study, define

$$\begin{aligned} Y_1 &= \alpha(\tau) \\ Y_2 &= \frac{d}{d\tau}\alpha(\tau) \\ Y_3 &= X(\tau) \\ Y_4 &= \frac{d}{d\tau}X(\tau) \end{aligned} \tag{27}$$

and

$$\begin{aligned} F_1 &= Y_2 \\ F_2 &= \frac{d^2}{d\tau^2}\alpha(\tau) \\ F_3 &= Y_4 \\ F_4 &= \frac{d^2}{d\tau^2}X(\tau) \end{aligned} \tag{28}$$

Equations 25 and 26 can thus be restated

$$F_2 - \cos(Y_1)F_4 = \eta_1 - \cos(Y_1) \tag{29}$$

$$-F_2\cos(Y_1)\eta_3 + F_4 = 1 + \eta_5 - \eta_2 Y_4 - {\eta_4}^2 Y_3 - {Y_2}^2 \sin(Y_1)\eta_3 \tag{30}$$

and solved for the second derivatives

$$F_2 = \frac{\eta_1 - \cos(Y_1) + \cos(Y_1)\left(1 + \eta_5 - \eta_2 Y_4 - {\eta_4}^2 Y_3 - {Y_2}^2 \sin(Y_1)\eta_3\right)}{1 - (\cos(Y_1))\,\eta_3} \tag{31}$$

$$F_4 = \frac{\eta_3 \cos(Y_1)\,(\eta_1 - \cos(Y_1)) + 1 + \eta_5 - \eta_2 Y_4 - {\eta_4}^2 Y_3 - {Y_2}^2 \sin(Y_1)\eta_3}{1 - (\cos(Y_1))^2\,\eta_3} \tag{32}$$

Some of the input parameters–direct and indirect–are given in Table 2. Some notes on these parameters are as follows:

1. The values for RPM_1 and RPM_2 were actually computed from physical parameters. The values for RPM_1 were be computed from Equations 3 and 10. The values for RPM_2 come from Equations 4 and 10.

Table 2
Other Parameters for Impact-Vibration Hammers

Model	RPM_1	RPM_2	n	i_{design}	F_{dyn}, kN	η_1
S-834	66.15	260.9	8.53	2	54.39	2.05
S-467M	59.55	245.4	12.69	2	236.47	1.95
S-402A	78.4	260.5	8	2	22.32	1.01
SP-53	49.2	221.4	4.95	1	388.39	0.55
S-836	60.0	252.0	10.57	2	145.23	1.85

2. The values of RPM_1 are high because they do not include the inertia of the shafts as they pass through the motors, or (in the case of SP-53) the gear mechanism.

3. Notes on η and related values are as follows:

- The values of η_1 shown in Table 2 are from the original power and eccentric moment specifications. The model attempts to match a value of η_1 with the given RPM_3.
- Based on considerations of Equation 18, $2.5 \leq \zeta \leq 25$ for all machines. The value of η_2 are then computed from Equation 15.
- Values for n are input into the model via η_3, which is computed from Equation 23. It is based on the target rotational speed of the machine RPM_3 and not the value the model produces.
- The value of η_4 can be computed from Equation 5 and the data given in Table 2.
- We discussed determining η_5 earlier.

4. The quantity i_{design} generally comes from the specifications; the model will confirm whether this is being simulated.

Once these equations are formulated and entered into the routine, along with the initial data, the solution is determined as follows:

1. A starting value for torque ratio is determined. To obtain this result, the first run assumes $\eta_1 = 1.1$ and the machine is simulated until it obtains a steady rotational speed of the eccentrics. As was the case with Tseitlin et al. (1987), this is done using least squares analysis and obtaining a weighted average RPM_3, although the implementation was a little more advanced.

2. If the average rotational speed thus obtained is above the target, the analysis is stopped. If it is above the target, it is repeated for a series of η_1 values until is increased until the resulting RPM_3 is above the target. At this point we have bracketed the final result between two values.

3. A regula falsi method, using η_1 as the input variable, is employed until RPM_3 is as close to the target angular velocity as the model will permit. How close that is depended on a number of factors. It is possible for $\eta_1 < 1.1$ but this did not take place.

4. Once a best case is obtained, the program returns values for such parameters as i, V_1, and N.

Energy and Power Output

Once these equations are solved and run, there are two things that need to be determined: a) the energy per blow of the ram and b) the power required to run the machine. These are a result of our analysis; it is certainly possible to use this to design by optimisation. However, the VNIIstroidormash designers did not have this kind of tool at their disposal. How did they determine the basic parameters of the machine?

The evidence at our disposal is incomplete but we can start by considering the fact that the free-hanging peak velocity of the ram is given by the equation

$$V_2 = \frac{g_c n}{\omega_3} \tag{33}$$

It can be shown that, by combining this and Equation 20 into the equations they actually used, this was a starting point for determining the velocity at impact. For the S-402A (Petrushkin, Friedman, Morgailo, and Krakinovskii (1966)) and S-834 (Petrushkin et al. (1964)) machines, the ratio between their estimated impact velocity and V_2 can be given by the equation

$$\frac{V_1}{V_2} = 2\,\frac{1}{(1-\xi^2)\,(1-R)} \tag{34}$$

where

$$R = \frac{V_1'}{V_1} \tag{35}$$

A different formulation of this was used for the S-467M (Petrushkin, Friedman, and Antinov (1967),) thus

$$\frac{V_1}{V_2} = 2\,\frac{\sqrt{1+R}}{\sqrt{1-R}\,(\xi^2-1)} \tag{36}$$

The two give similar results and in the case of $R = 0$ they are identical, with $\frac{V_1}{V_2} = 2.133$ for the case of $i = 2$.

Once the impact velocity is determined, the rated striking energy of the hammer (rated because there are no losses included) can be computed as

$$E_r = \frac{MV_1^2}{2} \tag{37}$$

The power required for this is given as

$$N_{impact} = \frac{E_r RPM_4}{60} \tag{38}$$

That power must come from the rotating eccentrics, which is given by the equation

$$N_{torque} = T\omega_3 = \eta_1 K g_c \omega_3 \tag{39}$$

Without consideration of losses,

$$N_{torque} = N_{impact} \tag{40}$$

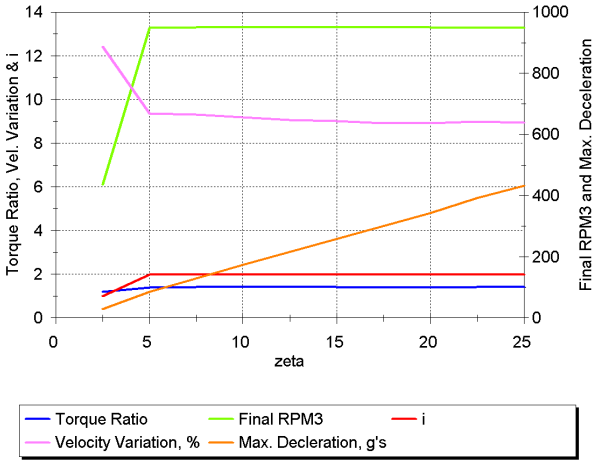

Figure 11. Graphed Results for S-834 Hammer

In the model under consideration, the impact velocity V_1 is a result of the analysis and not an input parameter, strictly speaking. The model computes both sides of Equation 40. Although they are the same in theory, in practice it is difficult to determine an exact value for V_1 because time discretisation makes it difficult to determine the velocity at the precise impact.

Results of the Model Survey

The model run, the data from it can be analysed. There are two ways of doing it, depending upon the data:

1. Graphed varying with ζ as $2.5 \leq \zeta \leq 25$ in increments of 2.5; and

2. Taking the maximum value from the survey and comparing them in scalar numbers.

Some sample time history data is also presented.

Graphed Data

The critical results are graphed in Figures 11, 12, 13, 14 and 15. Torque ratio η_1, variation in velocity, and rotational/impact frequency ratio i are plotted on the left y-axis. RPM_3 and maximum deceleration n_{impact} are plotted on the right y-axis.

The following can be observed, based on the results:

1. The least satisfactory results took place at the lower values of ζ; in fact, for S-402A (Figure 13) $\zeta = 2.5$ did not return a result at all. This could have been remedied had the torque been adjusted at zero and low rotational speeds, but it was not. Once the result got past this, the results became more consistent. With SP-53 the results for $\zeta = 2.5$ and $\zeta = 5$ were unsatisfactory; these were not considered further. It should be noted that the value of ζ for 150g impact deceleration is considerably higher than for the other machines.

2. The velocity variation is the ratio of the peak-to-peak difference of the rotational velocity of the eccentrics to the

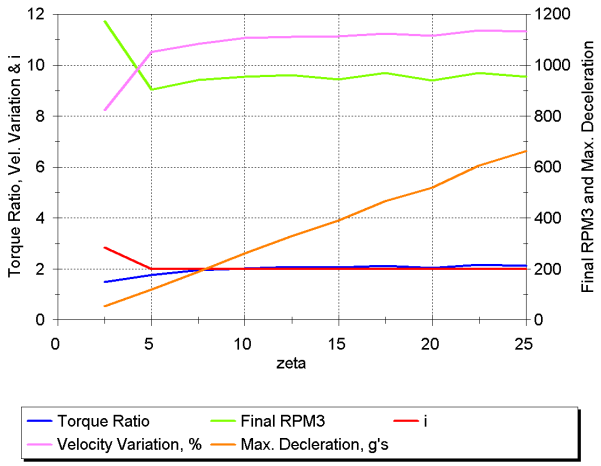

Figure 12. Graphed Results for S-467-M Hammer

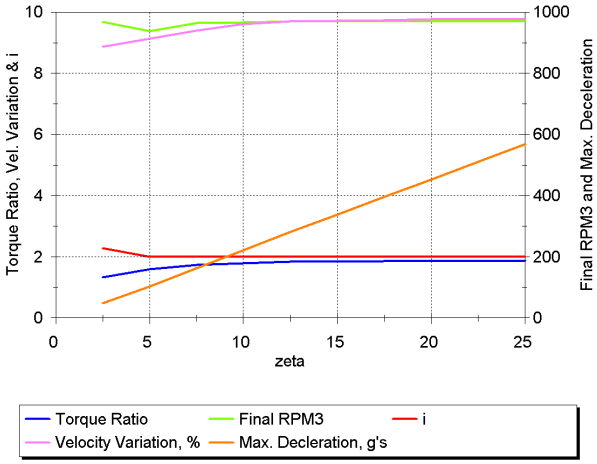

Figure 15. Graphed Results for S-836 Hammer

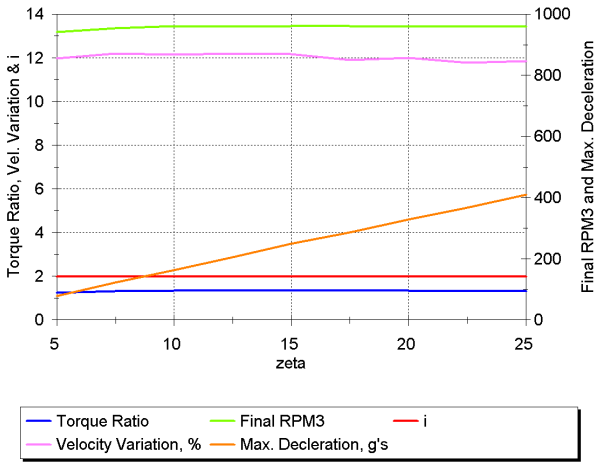

Figure 13. Graphed Results for S-402A Hammer

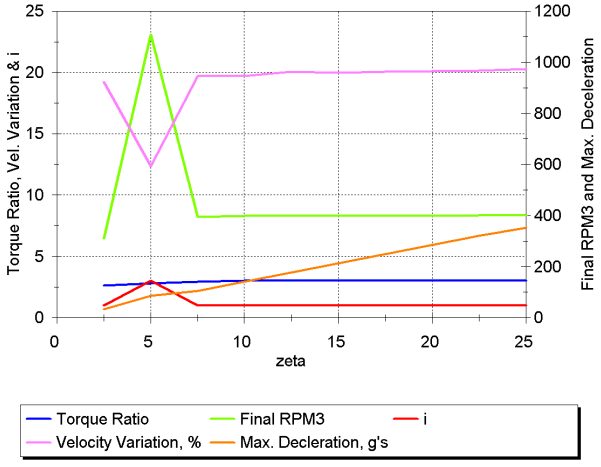

Figure 14. Graphed Results for SP-53 Hammer

least squares average of RPM_3, expressed as a percentage. Except for the SP-53, which is an outlier in many respects, this varies between 9-12% in the higher values of ζ. Given that this includes the effect of impact on the rotation of the eccentrics, this is not that great of a variation. It justifies the use of a constant rotational speed as a first analysis assumption. It is also worth noting that RPM_3 itself stabilised with higher values of ζ, although it did not always correspond exactly with the design rotational frequency. This suggested that some optimisation of other parameters is in order or, alternatively, that the design rotational frequency requires alteration.

3. The values of i are consistent with the original design parameters, and the replication of this phenomenon was a confirmation both of the phenomenon and of the model. Except for the SP-53, $i = 2$.

4. Torque ratio values generally stabilised when $\zeta \geq 15$. The lack of rebound doubtless contributed to that consistency.

5. The maximum deceleration varies linearly with ζ. The deceleration is computed by Equation 17. The value of M is a constant for each machine. The impedance Z is computed by Equation 13, where M and ω_3 are constants for a machine, and ζ increases. This means that the impact velocity is fairly consistent and that the deceleration varies with the impedance. A problem with this result is that the 150g limit on n_{impact} generally occurs in a fairly narrow range of value for ζ, a range bracketed by stability problems in the lower ranges of this parameter. This emphasises the need for careful design of the ram-pile interface to insure both ram deceleration within design parameters and stable operation. The impact model for this study is a simplistic one but lent itself to parametric study. It may also be too rigid; the ram, for example, is rigid in the model, something it is not in operation.

Because of the nature of the remaining data for this pro-

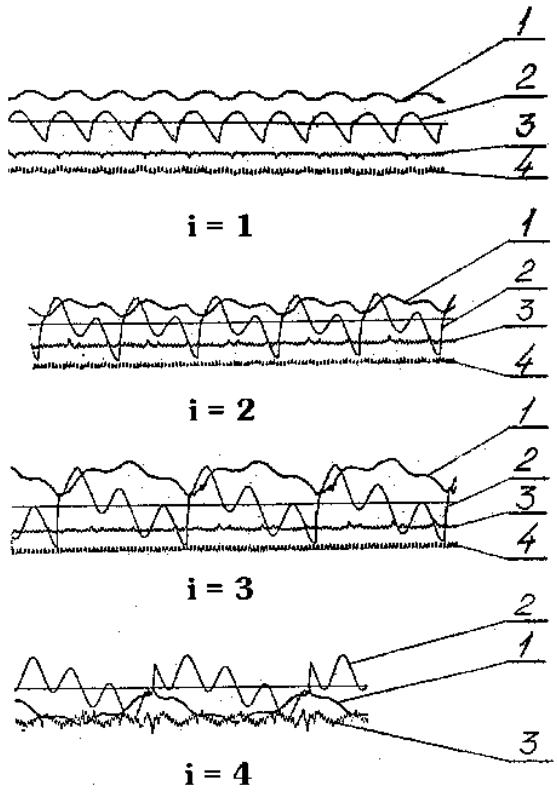

Figure 16. Strip Charts of the Basic Parameters of an Impact-Vibration Hammer for Various Values of i (from Warrington and Erofeev (1995))
Key: 1) displacement of the ram, 2) velocity of the ram, 3) angular position of the eccentric, 4) time marker

gram, it is difficult to make meaningful quantitative comparisons between the original performance and the results of the model. One place where a qualitative result can be obtained is in comparing original displacement and velocity time histories of the ram and those results from the model. This is done with original data in Figure 16 and model results in Figure 17.

The comparison of the two shows that the model replicates the basic displacement-time trace of the original at the same value of i. The velocity-time trace is more "rounded" at impact in Figure 16 than in Figure 17. This is because of the nature of the simulation of the resistance at impact and the high value of ζ.

It is not terribly rigourous, but another comparison can be made with the chalk trace shown in Figure 18. This is on the imact-vibration hammer VI-833A, intended for steel piling. Specifications are shown in Table 3. Unfortunately we do not have any further information to perform the analysis such as we have done on the other machines. Doing a chalk trace has been a common way to check the amplitude of a vibratory driver; in this case it also shows the irregular displacement-

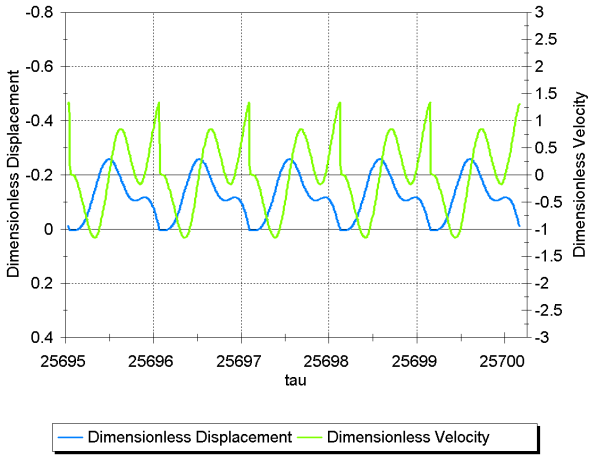

Figure 17. Ram Displacement and Velocity from Model, Consistent Operation, S-402A, $i = 2$, $\zeta = 25$

Table 3
Specifications for VI-833A Impact-Vibration Hammer

Parameter	Specification
Power	$44\,kW$
Impact Energy	$5.5/7.5\,kJ$
RPM_4	$330/245\ \frac{impacts}{minute}$
Ram weight	$3300\,kg$
Total weight	$6750\,kg$
Dimensions	$255 \times 144 \times 113.5\,cm$

time trace of the ram as well.

Another interesting result is the angular velocity of the eccentrics at the same interval of time, shown in Figure 19. While the variations are important–especially around impact–it should be noted that the range of angular velocities is relatively narrow, as was observed earlier. It is also probable that the stiffer impact of the model noted in the previous comparison may influence the results here as well.

Comparison of Scalar Results

Some of the results are best compared by taking the maximum value of the results and comparing them with original specifications. Some of these are presented here.

Torque Ratio. The comparison of torque ratio and power characteristics are shown in Table 4.

Using η_1 is the simplest way to make this comparison, as the model was able to achieve a value of RPM_3 close to specifications. The results show that, except for S-834, the torque generated by the motors is below that predicted by the model. The difference may be due to the fact that, in some cases, the machines were designed with rebound energy using R. In the case of SP-53 the difference was substantial, and this will be discussed below.

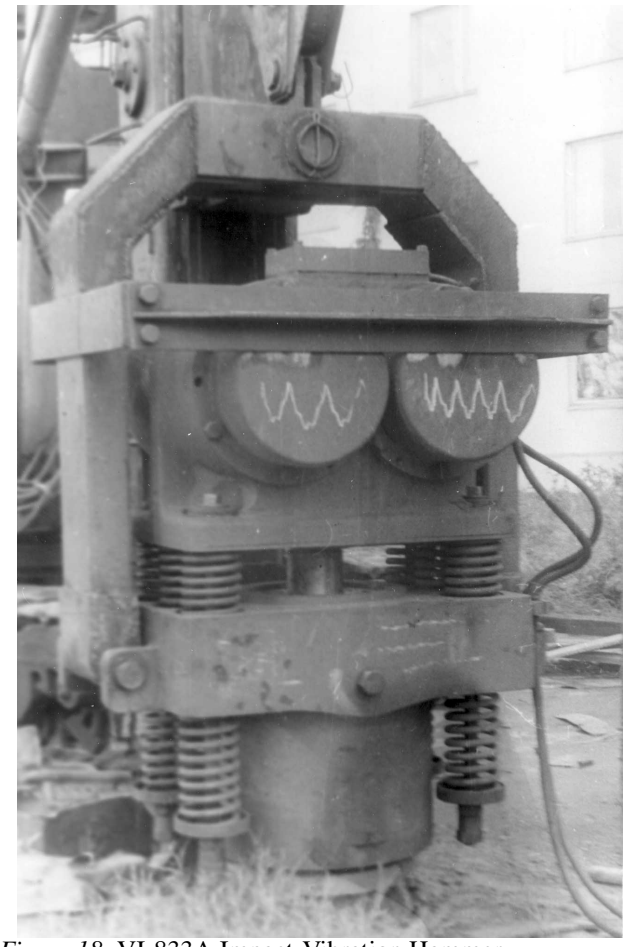

Figure 18. VI-833A Impact-Vibration Hammer

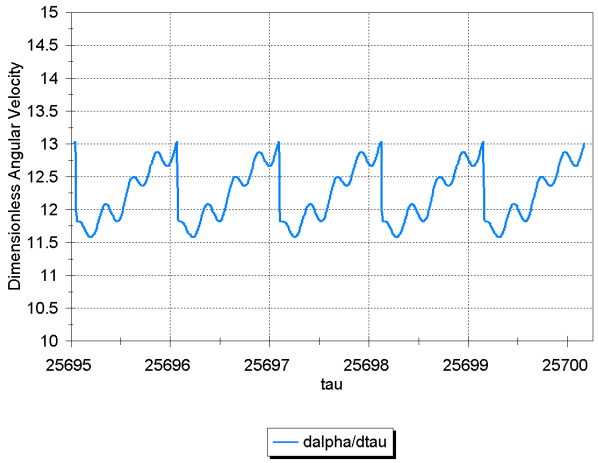

Figure 19. Angular Velocity as a Function of Dimensionless Time, S-402A, $i = 2$, $\zeta = 25$

Table 4
Torque Ratio Comparison

Model	η_1 from Specifications	η_1 from Model
S-834	2.05	1.44
S-467M	1.95	2.17
S-402A	1.01	1.36
SP-53	0.55	3.05
S-836	1.85	1.87

Table 5
Impact vs. Torque Power

Model	N_{torque}, kW	N_{impact}, kW
S-834	7.72	7.63
S-467M	48.44	50.71
S-402A	2.96	2.96
SP-53	278.0	294.9
S-836	26.26	27.06

Impact vs. Torque Power. Applying the model results to Equations 27, 28 and 29 yields results as shown in Table 5. In theory the two should be identical; as other losses are not included in this model. However, as noted earlier, perfect correspondence between the two cannot be expected since the "impact velocity" used is actually just before impact. The two powers are reasonably close, considering these factors.

Minimum Machine Dead Weight Requirement. An impact-vibration hammer with a sprung suspension is a machine with downward assist for the ram. Downward assist is generally provided by a force exerted by the ram pushing upward on the dead weight of the hammer frame. For most impact hammers, this force is generally furnished by a pressurised gas, either the air or steam that powers the hammer (Vulcan, Raymond, Conmaco, MKT,) hydraulic fluid acting downward (Junttan,) trapped air or nitrogen that is compressed by the upward motion of the ram (IHC, Link-Belt) or a combination of these. With the impact-vibration hammer the spring system provides downward assist to gravity. The shorter the stroke of the ram from maximum upward distance from impact, the larger the dead weight or other downward assist necessary to prevent the frame from coming up during operation.

The model tracked the maximum upward displacement of the ram and, multiplying this by the spring constant, estimated the minimum weight required to keep the frame stable during operation. This is shown, and comparison with the original specifications is given, in Table 6.

Except for the S-402A, none of the machines has adequate deadweight in the frame for stable operation. There is considerable evidence that VNIIstroidormash researchers wrestled with this problem, including using a clamp to fix the frame to the pile or adding bias weights to the frame (see Figure 8.) Simply increasing the frame weight renders the

Table 6
Frame Dead weight Comparison

Model	Estimated Min. Frame Weight, kg	Actual Frame Weight, kg
S-834	2,027	1,150
S-467M	7,822	4,600
S-402A	812	886
SP-53	38,257	3,000
S-836	5,144	3,100

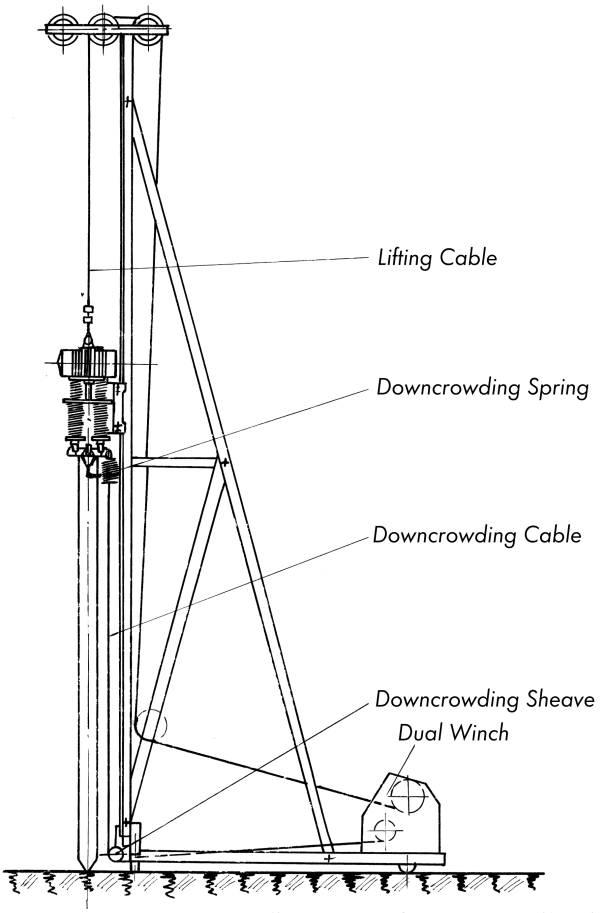

Figure 20. Down Crowding Setup for Impact-Vibration Hammer (from Petrushkin et al. (1964))

machine heavier to handle (Warrington and Erofeev (1995).) Other solutions include down crowding or pulling the machine to increase its apparent weight; this is shown in Figure 20. With the increase in the use of rigs even in the U.S., this has become a more viable option. It is not too much of a stretch to see this hammer used in, say, an excavator mast rig, such as is shown in Figure 21 with a Vulcan impact hammer. It is worth noting that the VI-833A model (Figure 18) had the option of being mounted on an excavator.

Length and Impact Power. In any effort to evaluate the advantages and disadvantages of the impact-vibration hammer with other impact equipment, the differences in impact velocity and frequency need to be considered. As a general rule, the impact-vibration hammers impact the pile with lower velocity (and thus energy) and higher frequency blows that conventional impact hammers. A quick survey impact power output (using Equation 38) is shown in Table 7.

Figure 21. Excavator Mast Rig with Vulcan Impact Hammer (photo courtesy of Jonathan Tremmier, Vulcan Foundation Equipment)

An additional information item in Table 7 is the overall length of these hammers. In both cases the specifications for the VNIIstroidormash hammers come from either the model (power output) or the specifications given either in their technical documentation or in Warrington and Erofeev (1995). For the Vulcan and MKT hammers, the specifications came from Warrington (2011). For Pileco and IHC hammers, specifications come from their respective manufacturer's data.

From these results we can note the following:

1. The power range of the impact-vibration hammers under study is comparable with those of hammers in common current use.

2. The length of the impact-vibration hammers is considerably less than comparable conventional impact hammers. This is especially true for the Pileco (and other diesel) and IHC hammers. This can be very important in the adaptation of these hammers to pile driving rigs, especially those mounted on excavators and other general types of construction equipment, as extended hammer length reduces the overhead available for pile length. This is especially critical in applications where headroom is restricted by the job conditions.

Table 7
Power Output and Length Data for Various Impact and Impact-Vibration Hammers

Manufacturer	Model	Power Output, kW	Length, cm
Vulcan	DGH-100	2.64	127
VNIIstroidormash	S-402A	2.96	104
VNIIstroidormash	S-834	7.63	135
Vulcan	#1	20.34	396
Vulcan	DGH-900	21.51	206
Pileco	D12-42	24.95	585
VNIIstroidormash	S-836	27.06	187
MKT	9B3	28.67	249
MKT	10B3	31.08	285
IHC	S-30	32.50	591
Pileco	D18-42	35.52	585
MKT	11B3	42.61	338
Vulcan	50C	44.36	310
Pileco	D25-32	48.74	649
VNIIstroidormash	S-467M	50.71	194
IHC	S-70	58.33	705
Pileco	D30-32	58.46	649
VNIIstroidormash	SP-53	294.86	340

3. How comparable two hammers with similar impact power but different proportion between blow rate and striking energy are in actual pile driving conditions depends upon the type of pile and soil being driven into; nevertheless, the possibility of using a low-headroom electric machine has some significant potential. VNIIstroidormash researchers were aware of this difference (Warrington and Erofeev (1995)):

> This hammer also addressed the builders' need for the driving of reinforced concrete piles and cylinder piles not only in loose soils but also in firmer ones, such as clay soils. Although they were used during the early stages of their development only in loose, water-saturated (sandy, muddy, etc.) soils, at the present time it is necessary to use them also in stiff soils of medium density (loamy, plastic-clayey, dry sandy and gravelly soils.)

The Case of the SP-53. It should be evident by now that the SP-53 is the "outlier" of the group in just about every respect. So some comments are in order about this machine.

The SP-53 was considerably larger than the other machines under consideration. Additionally it had a gear-driven speed reducing mechanism so that, while for the motor $RPM_3 = 980$, for the eccentrics the rotational speed was 400 RPM. One of the important results of the model was that likewise $RPM_4 = 400$; the specifications were not clear on this point.

The torque ratio for the machine based on the 50 kW power specification was 0.55 as shown in Table 4. This is based on RPM_4 (as opposed to RPM_3 for the other machines) so to be directly comparable to the other values of η_1. Although starting (zero RPM) torque for electric motors of the kind is higher than the steady-state torque, in order for the eccentrics to go "over centre" the torque ratio would have to be around twice its current value. This is attainable under certain circumstances. The larger problem, however, is that the model, which tracks the power specification reasonably well for the other machines, indicates that the torque ratio from the model at RPM_3 is approximately six times the ratio indicated in the specifications.

At this point there are too many discrepancies in the data we have to make definite conclusions about this machine. One thing that is evident, however, is that with this machine and the VI-571 VNIIstroidormash researchers had as their objective the solution of several of their problems (Warrington and Erofeev (1995).) These include the aforementioned weight/down-crowding issue and the issue of varying soils, but it also include two other important capabilities: a) the ability to operate either as a vibratory driver or impact-vibration hammer, and b) the ability to change the machine's operation by applying bias loads to the springs and thus altering the clearance. In the case of the VI-571, these were accomplished hydraulically; with the SP-53, these were accomplished using an electromagnet.

Impact-Vibration Sheet-Pile Extractor. Although the impact-vibration hammers for driving were discontinued, one application that was continued was the sheet pile extractor, an example of which is shown in Figure 22. Specifications are shown in Table 8. In spite of the advance that vibratory driving made for the installation and removal of sheet piles (and other piles as well) there were and are those cases where vibrations do not generate large enough forces to allow for extraction. This includes cases where the interlocks are severely damaged or clogged. This hammer would compete with air extractors (such as the Vulcan and MKT extractors) and hydraulic ones as well. The striking energy is above that of a Vulcan 1200A extractor (see Table 3) and the blow rate is comparable as is the weight. The clamp should be noted; it (or some kind of connection capable of upward force transmission) is mandatory for an extractor, as is the additional suspension to allow the crane to pull the machine and pile upward.

Discussion

1. Except for the SP-53, the model was capable of replicating the data we have on these machines to a reasonable degree. This suggests that we can alter design parameters and improve the design that we have. This is beyond the scope of the paper.

2. The best replication we received in the model is the rep-

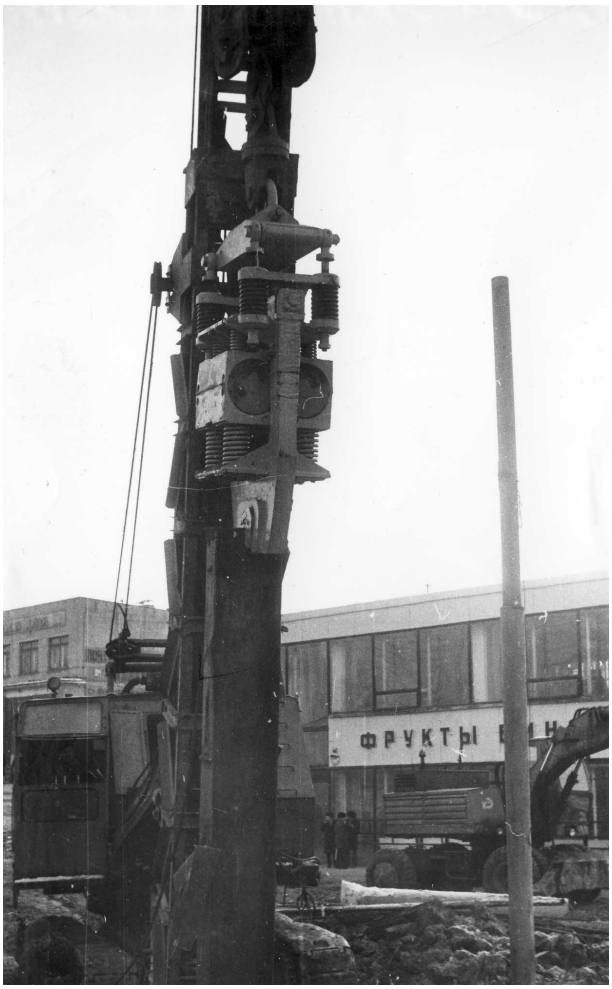

Figure 22. SP-83 Sheet Pile Extractor (from Warrington and Erofeev (1995))

lication of i; this was a crucial result. Other important parameters include the maximum deflection of the springs and the impact velocity of the ram.

3. Probably the least satisfactory aspect of the model is the way it attempts to simulate impact. A purely impedance based method of simulating impact is too simplistic.

4. Whether we should consider the effect of rebound is an open question. It is certainly possible to obtain rebound from a semi-infinite pile model (Warrington (1987, 2020).) The key questions are a) how does rebound affect the motion of the ram and b) how does it affect the power requirements of the machine. For some of the original machines $R = 0.12$ which means that the rebound energy of the impact energy is $R^2 = 0.12^2 = 0.0144$ or 1.44%. This not a very large portion of the impact energy coming back from the pile.

5. Although it is possible–and certainly has been done–to simulate the system using a fixed angular velocity of the eccentrics since the variable $\frac{d}{dt}\alpha(t)$ model has been developed, there is little incentive to revert to a model where $\frac{d^2}{dt^2}\alpha(t) = 0$.

Table 8
Specifications for SP-83 Sheet Pile Extractor, Compared with Vulcan 1200A Extractor

Specification	SP-83	Vulcan 1200A
Tons of Sheeting Extracted, $\frac{tons}{hour}$	6.5	-
Impact Energy, kJ	2.85	2.2
RPM_4, $\frac{impacts}{minute}$	480	540
Impact Force, kN	240	-
Power, kW	34	-
Dimensions, cm	$137 \times 96 \times 275$	$114 \times 102 \times 305$
Weight w/o Control Panel, kg	4900	4173

6. The use of impact power as a way of comparing hammer performance needs to be considered in light of soil and pile type, especially the former.

7. The model was not used to analyse different values of spring bias, although that option is possible for future study.

8. The VI-571 and SP-53 impact-vibration hammers introduce the possibility of one machine capable of both vibrating and impacting the pile. This would be advantageous in the case of a) using the impact mode to evaluate the static capacity of the pile and b) to enable to machine to continue to move the pile when vibratory driving mode no longer progresses the pile. The former is problematic because it is entirely possible that the reduction in shaft resistance due to vibrations will be quantified in the near future, and in any case it is not clear whether switching into impact mode will reduce the effects on horizontal soil stresses. The latter is a useful feature, but care must be taken not to make the equipment excessively complex and by doing so compromise its reliability.

9. One of the great challenges of these machines is to extend their life (bearings, ram points, ram frames, etc.) This was not directly considered in this study. One thing that needs to be considered going forward is how advances in materials and components can extend the life of these machines.

10. For this type of machine to be introduced in current circumstances, it would be necessary to include both comprehensive control and monitoring systems (especially of the impact velocity.) Including these would both give the user more control over the operation of the machine and the inspector the necessary information to evaluate the performance of the machine relative to axial pile capacity.

Conclusion

The impact-vibration hammers are an interesting part of the history of pile driving equipment, but they were ultimately set aside by the place that developed them for more conventional types. Development of the parametric model shown in this study indicates that they can be simulated–and their parameters studied–in ways that can lead to the ad-

vancement of this equipment. With the renewed interest in electric equipment, perhaps the time has come for these machines to once again take their place in the field of deep foundations.

Nomenclature

$\alpha(t)$ Angle of eccentrics, radians

β Stiffening coefficient, generally 1.2

η_1 Torque ratio

η_2 Impedance ratio in terms of pendulum frequency

η_3 Ram acceleration due to rotation of eccentrics in terms of pendulum frequency

η_4 Ratio of natural to pendulum frequency

η_5 Bias ratio

ω_1 Pendulum Frequency, rad/sec

ω_2 Natural Frequency, rad/sec

ω_3 Angular velocity of eccentrics, rad/sec

ω_4 Impact frequency, rad/sec

τ Dimensionless time

ξ Ratio of natural frequency to eccentric angular velocity

ζ Impedance ratio

E_r Rated striking energy of ram, J

$F_{1,2,3,4}$ First derivatives for Runge-Kutta scheme

g_c Gravitational constant = $9.81 \frac{m}{sec^2}$

i Ratio of eccentric angular velocity to impact frequency

I_o Mass moment of inertia of eccentrics, $kg - m^2$

i_{design} Design ratio of angular velocity of eccentrics to impact frequency

K Eccentric Moment, kg-m

k Spring constant, N/m

M Ram Mass, kg

n Acceleration of the ram due to rotation of the eccentrics, g's

N_{impact} Power from impact, W

n_{impact} Peak deceleration of ram at impact, g's

N_{max} Design deceleration of the ram at impact, usually 150 g's

N_{rat} Power of motors from specifications, kW

N_{torque} Power from torque, W

Q_{vp} Bias force/preload of springs, N

R Stroke speed restoration coefficient

RPM_1 Pendulum frequency of eccentrics, RPM

RPM_2 Natural frequency of spring-ram mass system, RPM

RPM_3 Frequency of eccentric rotation, RPM

RPM_4 Impact Frequency, RPM or impacts/minute

T Torque, J

t Time, seconds

V_1' Rebound velocity of ram after impact, m/sec

V_1 Impact velocity of ram, m/sec

V_2 Free hanging, impactless peak velocity of ram, m/sec

$V_{1_{max}}$ Maximum impact velocity, usually 2 m/sec

$X(\tau)$ Dimensionless ram displacement

$x(t)$ Displacement of ram, m

$Y_{1,2,3,4}$ Functions for Runge-Kutta scheme

Z Effective impedance of pile, $\frac{N-sec}{m}$

Z_o Clearance between ram and anvil, m

F_{dyn} Dynamic force of eccentrics, N

References

Barkan, D. (1957, August). Foundation and drilling by the vibration method. *Proceedings of the Fourth International Conference on Soil Mechanics and Foundation Engineering*, *2*, 3–7.

Erofeev, L., Smorodinov, M., Fedorov, B., Vyazovkii, V., & Villumsen, V. (1985). *Maschini i oborudanie dlya ustroiva osnovanii i fundamentov (machines and equipment for the installation of shallow and deep foundations)* (Second ed.). Moscow, USSR: Mashinostrenie.

Goble, G., & Rausche, F. (1976). *Wesweap – wave equation analysis for piles* (Vols. Vol. I, Background, FHWA-IP-76-14.1, Vol. II, Users Manual, FHWA-IP-76-14.2, Vol. III, Program Documentation, FHWA-IP-76-14.3, Vol. IV, Narrative Presentation, FHWA-IP-76-14.4). U.S. Army Engineer Waterways Experiment Station, Geotechnical Laboratory.

Isaacs, D. (1931, September). Reinforced concrete pile formulae. *Journal of the Institution of Engineers Australia*, *3*(9), 305–323.

Ivanov-Smoleksky, A. (1982). *Electrical machines* (Vol. 2). Moscow, USSR: Mir Publishers.

Massarsch, K. (2023). Soil resistance during vibratory driving in sand. *Proceedings of the Institution of Civil Engineers: Geotechnical Engineering,*. doi: 10.1680/jgeen.22.00193

Massarsch, K., & Fellenius, B. (2020). Deep compaction of sand causing horizontal stress change. *Geotechnical Engineering Journal of the SEAGS & AGSSEA*, *51*(2), 9-21.

Petrushkin, L., Friedman, I., & Antinov, B. (1967). *Vibromolot s-467m: Raschetno-poyasnitelnaya zaniska i instruktsita po ekspluatatsii, rabotsii proyekt (impact-vibration hammer s-467m: Calculational and explanatory statement and instructions for operation, work project)* (Tech. Rep.). Moscow, USSR: VNIIstroidormash.

Petrushkin, L., Friedman, I., & Morgailo, V. (1964). *Vibromolot s-834: Vremennaya instruktsiya po ekspluatatsii (impact-vibration hammer s-834: Provisional instructions for operation)* (Tech. Rep.). Moscow, USSR: VNIIstroidormash.

Petrushkin, L., Friedman, I., Morgailo, V., & Krakinovskii, L. (1966). *Vibromolot s-402a: Raschet (impact-vibration hammer s-402a: Calculation)* (Tech. Rep.). Moscow, USSR: VNIIstroidormash.

Rebrik, B. (1966). *Vibrotekhnika v burenii (vibro-technology for drilling)*. Moscow, USSR: Nedra.

Savinov, O., & Luskin, A. Y. (1960). *Vibratsionnyy metod pogruzheniya i yego primeneniye v stroitel'stve (vibratory method of installation and its application to construction)*. Leningrad, USSR: Gosstroyizdat.

Smith, E. (1960). Pile driving analysis by the wave equation. *Journal of the Soil Mech. Found. Eng. Div., ASCE*, *86*.

Tseitlin, M., Verstov, V., & Azbel, G. (1987). *Vibratsionnaya tekhnika i tekhnologiya v svainykh i burovikh rabotakh (vibratory methods and the technology of piling and boring work)*. Leningrad, USSR: Stroiizdat, Leningradskoe Otdelenie.

Warrington, D. (1987, April). A proposal for a simplified model for the determination of dynamic loads and stresses during pile driving. *Proceedings of the Offshore Technology Conference*, 329–338. doi: 10.4043/5395-MS

Warrington, D. (1992, October). Vibratory and impact-vibration pile driving equipment. *Pile Buck*(Second Issue), 2A–28A.

Warrington, D. (1994, August). Survey of methods for computing the power transmission of vibratory hammers. *Pile Buck*(Second Issue).

Warrington, D. (2006, September). Development of a parameter selection method for vibratory pile driver design with hammer suspension. *Colloquium of the Department of Mathematics of the University of Tennessee at Chattanooga*.

Warrington, D. (Ed.). (2011). *vulcanhammer.info guide to pile driving equipment* (Second ed.). pz27.net.

Warrington, D. (2020). *Otc 5395 revisited: Analysis of cushioned pile hammers* (Tech. Rep.). University of Tennessee at Chattanooga. doi: 10.13140/RG.2.2.10487.04002/1

Warrington, D. (2021, April). *Reconstructing a soviet-era plastic model to predict vibratory pile driving performance* (Vol. 2021 ReSEARCH Dialogues Conference; Tech. Rep.). Chattanooga, TN: University of Tennessee at Chattanooga. doi: 10.13140/RG.2.2.30320.38403

Warrington, D. (2022, March). *Inclusion of rotational inertial effects in power consumption calculations for vibratory pile equipment* (Tech. Rep.). Chattanooga, TN: Affiliation: University of Tennessee at Chattanooga. doi: 10.13140/RG.2.2.30074.36805

Warrington, D., & Erofeev, L. (1995, May). Russian impact-vibration pile driving equipment. *Pile Buck*, *May*(2), 4A-19B. Retrieved from `https://wp.me/p8QSbh-RF`

Warrington, D., Nifontov, V., Erofeev, L., & Trifonov-Yakovlev, D. (1997, September 2). *Sea water pile hammer* (patentus No. 5662175). Chattanooga, TN.